Model Predictive Control of Cascaded Multilevel Battery Assisted Quasi Z-Source PV Inverter with Reduced Computational Effort

Lashab, Abderezak; Séra, Dezso; Guerrero, Josep M.

Published in:
Proceedings of 2019 IEEE Energy Conversion Congress and Exposition (ECCE)

DOI (link to publication from Publisher):
10.1109/ECCE.2019.8912551

Publication date:
2019

Document Version
Accepted author manuscript, peer reviewed version

Model Predictive Control of Cascaded Multilevel Battery Assisted Quasi Z-Source PV Inverter with Reduced Computational Effort

Abderezak Lashab, Dezso Sera, Josep M. Guerrero
Department of Energy Technology, Aalborg University, Aalborg DK-9220, Denmark
abl@et.aau.dk, des@et.aau.dk, joz@et.aau.dk

***Abstract*—In cascaded multilevel quasi Z-source inverters (CM-qZSI), the intermittent and stochastic fluctuation of the solar power injected to the grid can be smoothened by connecting a battery in parallel with one of the qZ network capacitors. However, since CM-qZSI is a special case of the single phase qZSI, it suffers from some of its demerits, such as double line-frequency ripple. This affects the battery current, the second qZ network's inductor current, and the qZ network's capacitor voltages. This issue can be alleviated either by increasing the size of the passive elements or by developing advanced control schemes, such as MPC. However, MPC is computationally intensive, especially in multilevel converters. In this paper, a low computational control method for PV-fed battery assisted CM-qZSI is proposed, where proportional-resonant (PR) controller is introduced in the control algorithm. The prediction is performed only for the dc side of the converter; hence, the algorithm iterates for the shoot through and zero states only. As shown in the obtained results, by using the proposed method, the double line-frequency ripple can be significantly reduced, while a less computational effort compared to the conventional MPC is needed.**

***Keywords*—Battery, Computational burden, Grid connected, Modular, MPC, MPPT, Photovoltaic, P&O, Z-network.**

I. Introduction

Nowadays, modular multilevel converters are the most adopted category for high- and medium-voltage applications, since a higher output voltage can be achieved by a series connection of identical power modules, in which low voltage semiconductor devices are used [1]-[2]. Modular multilevel converter topologies have several advantages such as low switching frequency, high output voltage quality allowing the use of a much less sizable output filter, reduced *dv/dt* leading to less electromagnetic interference (EMI), and fault tolerance [3].

CM-qZSI presents many advantages over the conventional multilevel converters when applied in photovoltaic (PV) power systems. For instance, the CM-qZSI provides a balanced dc-link voltages through its voltage boost ability, as well as saving one-third modules [4]. The qZS-CMI allows the integration of energy storage by adding a battery in each module to limit the ramp rate of the solar injected power to the grid, and to store the energy for other times.

A detailed controller parameter design for the three-phase CM-qZSI is demonstrated in [4] by using Bode plots. The authors in [5], proposed a control strategy for the three-phase CM-qZSI based on a modified space vector modulation. In [6], CM-qZSI has been used for improving the power quality in a single phase system. A maximum power point tracking (MPPT) algorithm based on automatic output power ratio constraint is developed in [7], to deal with the problem of the output current distortion in single phase CM-qZSI in case power mismatch among the submodules. In [8], the cascaded qZS inverter has been used in a different configuration—only one leg is used in each power submodule, and the total resulted dc-link voltage is inverted by using a low frequency inverter.

On the CM-qZSI with integrated energy storage, only a limited number of research papers have been introduced so far [9], [10], and [11]. The first control scheme of the battery assisted CM-qZSI has been introduced first in [9], where a Proportional Integral (PI) controller is used for regulating the PV voltage at its reference in each submodule, and one PR controller is used for the regulation of the injected current to the grid. The power delivered by each submodule is determined by using an energy management system by taking into account the extracted PV power and the state of charge (SoC) of the battery. Fuzzy Logic based control strategy has been proposed for the battery assisted CM-qZSI in [10]. In [11], a SoC balancing algorithm is presented, the algorithm is applied to CM-qZSI; however, it can be applied to any cascaded multilevel converter topology.

CM-qZSI suffers from a double line-frequency ripple, which is induced by the periodic instantaneous power delivery to the grid. In case of battery integrated CM-qZSI, this ripple appears in the battery current and voltage, which increases its internal resistance and fades its capacity. A way to mitigate this ripple is by using model predictive control (MPC). MPC is a powerful approach, but since it predicts the behavior of the controlled variable for all the possible switching states at each sampling time, it is computationally demanding.

In this paper, an MPC-based control strategy for the battery assisted CM-qZSI is proposed. The double line-frequency ripple in the battery current can be considerably mitigated, where less computational effort compared to the conventional MPC is applied.

II. The Configuration of the Cascaded Multilevel Quasi Z-Source Inverter with Battery Storage

An extended model of the PV fed Quasi Z-source cascaded multilevel inverter is shown in Fig. 1, where the second qZS

network capacitor in each submodule is paralleled to a battery. The qZS network is then connected to the dc-link of the conventional H-bridge. In addition to the two active states and the zero state of the H-bridge, a shoot through state is also possible in the qZS power module as shown in Fig. 2(c) [12]. The shoot through state consists of gating both switches in the same leg simultaneously. The aim of applying the later state is to boost the voltage at the dc-link of the H-bridge. During the shoot-though state, the qZS inductors charge at the expenses of the energy stored in the capacitors and from the power source, which is a PV array in this paper. As soon as the shoot through state ends, the energy stored in the inductors charges the capacitors, thus boosting their voltage.

The output voltage of the CM-qZSI as function of the dc-link voltages and switching states can be written as

$$v_{out}(t+T_s)=\sum_{i=1}^{n} v_{PNi}(S_{1i}-S_{2i}) \tag{1}$$

such as, v_{PNi} is the voltage at the dc-link of the i^{th} H-bridge, S_{1i} and S_{2i} are the switching states of the first and second leg of the *ith* H-bridge respectively. The output voltage as a function of the ac side parameters of the CM-qZSI can be assessed through Kirchhoff's voltage law as the following,

$$v_{out}=L_f\frac{di_g}{dt}+r_f i_g+v_g \tag{2}$$

where v_g, i_g, L_f, and r_f are the grid voltage, the current injected to the grid, the filter inductance, and the filter stray resistance.

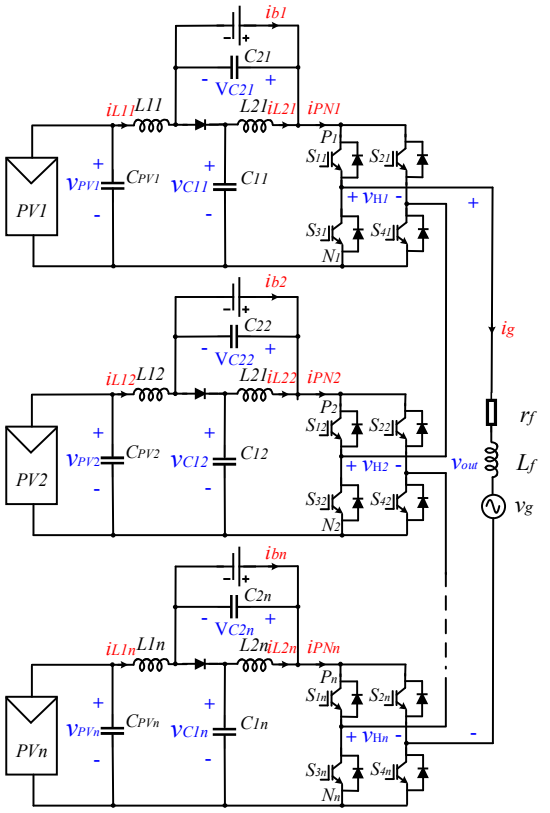

Fig. 1. PV fed Quasi Z-source cascaded multilevel inverter with integrated energy storage.

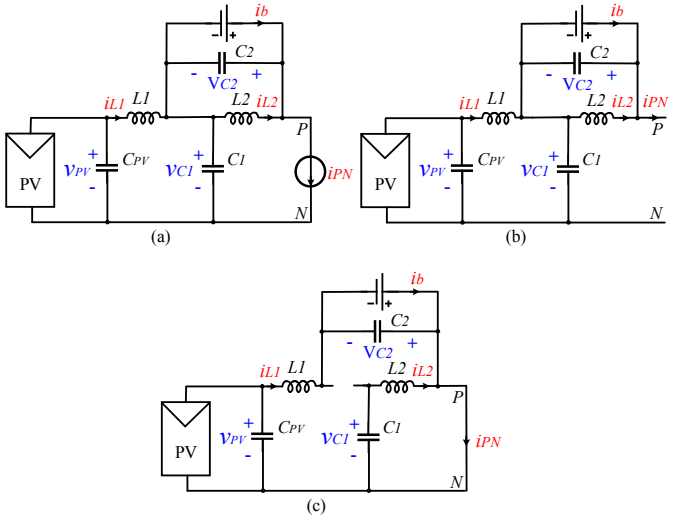

Fig. 2. PV fed Quasi Z-source submodule with integrated energy storage during: (a) active states, (b) zero state, and (c) shoot through state.

In what follows it is assumed that the qZS network passive elements in each submodule are symmetrical (C_1=C_2 and L_1=L_2) and the total number of power modules is three. Considering the qZS network's inductors currents, the first qZ network's capacitor voltage, and the battery voltage as the state variables, $\boldsymbol{x}$=[i_{L1}, i_{L2}, v_{C1}, v_{C2}]^t. The state space model of each submodule during the active states can be found as follows

$$\dot{\boldsymbol{x}}=\mathbf{A}_1\cdot\boldsymbol{x}+\mathbf{B}_1\cdot\boldsymbol{u} \tag{3}$$

such as:

$$\mathbf{A}_1=\begin{bmatrix} -\frac{r_{L1}}{L_1} & 0 & -\frac{1}{L_1} & 0 \\ 0 & -\frac{r_{L2}}{L_2} & 0 & -\frac{1}{L_2} \\ \frac{1}{C_1} & 0 & 0 & 0 \\ 0 & \frac{1}{C_2} & 0 & 0 \end{bmatrix};\ \mathbf{B}_1=\begin{bmatrix} \frac{1}{L_1} & 0 & 0 \\ 0 & 0 & 0 \\ 0 & 0 & -\frac{1}{C_1} \\ 0 & -\frac{1}{C_2} & -\frac{1}{C_2} \end{bmatrix};$$

$$\boldsymbol{u}=\begin{bmatrix} v_{PV} & i_b & i_{PN} \end{bmatrix}^t$$

From Fig. 2(b), the inductor voltages during the zero state are the same as in the active state; however, the capacitors currents change. The state space model can be expressed as:

$$\dot{\boldsymbol{x}}=\mathbf{A}_0\cdot\boldsymbol{x}+\mathbf{B}_0\cdot\boldsymbol{u} \tag{4}$$

where:

$$\mathbf{A}_0=\begin{bmatrix} -\frac{r_{L1}}{L_1} & 0 & -\frac{1}{L_1} & 0 \\ 0 & -\frac{r_{L2}}{L_2} & 0 & -\frac{1}{L_2} \\ -\frac{1}{C_1} & 0 & 0 & 0 \\ 0 & -\frac{1}{C_2} & 0 & 0 \end{bmatrix};\ \mathbf{B}_0=\begin{bmatrix} \frac{1}{L_1} & 0 & 0 \\ 0 & 0 & 0 \\ 0 & 0 & 0 \\ 0 & -\frac{1}{C_2} & 0 \end{bmatrix};$$

The state space model of each submodule during the shoot through state can be found similarly as follows

$$\dot{\boldsymbol{x}}=\mathbf{A}_{st}\cdot\boldsymbol{x}+\mathbf{B}_{st}\cdot\boldsymbol{u} \tag{5}$$

where:

$$\mathbf{A}_{st}=\begin{bmatrix} -\frac{r_{L1}}{L_1} & 0 & 0 & \frac{1}{L_1} \\ 0 & -\frac{r_{L2}}{L_2} & \frac{1}{L_2} & 0 \\ 0 & -\frac{1}{C_1} & 0 & 0 \\ -\frac{1}{C_2} & 0 & 0 & 0 \end{bmatrix};\ \mathbf{B}_{st}=\begin{bmatrix} \frac{1}{L_1} & 0 & 0 \\ 0 & 0 & 0 \\ 0 & 0 & 0 \\ 0 & -\frac{1}{C_2} & 0 \end{bmatrix};$$

The average state space model of each qZS submodule can be obtained through the average state approach as

$$\dot{\boldsymbol{x}}=\mathbf{A}\cdot\boldsymbol{x}+\mathbf{B}\cdot\boldsymbol{u} \tag{6}$$

such as

$$\mathbf{A}=\begin{bmatrix} -\frac{r_{L1}}{L_1} & 0 & \frac{D_i-1}{L_1} & \frac{D_i}{L_1} \\ 0 & -\frac{r_{L2}}{L_2} & \frac{D_i}{L_2} & \frac{D_i-1}{L_2} \\ \frac{2U_i+D_i-1}{C_1} & -\frac{D_i}{C_1} & 0 & 0 \\ -\frac{D_i}{C_2} & \frac{2U_i+D_i-1}{C_2} & 0 & 0 \end{bmatrix};\ \mathbf{B}=\begin{bmatrix} \frac{1}{L_1} & 0 & 0 \\ 0 & 0 & 0 \\ 0 & 0 & -\frac{U_i}{C_1} \\ 0 & -\frac{1}{C_2} & -\frac{U_i}{C_2} \end{bmatrix};$$

where U_i and D_i are the active state and shoot through state duty cycles in the *ith* submodule, respectively.

III. Conventional Control of Cascaded Multilevel Quasi Z-source Inverter with Battery Storage

The schematic of the conventional control of the battery assisted CM-qZSI for PV systems is shown in Fig. 3. The injected power from each submodule is determined based on the harvested power from the PV array and an energy management system (EMS) through its respective switching function (U_i). The switching function that is fed to the EMS is the output of a PR controller, which is used to regulate the grid current to its reference. The harvested power from the PV array in the i^{th} cell is maximized by using a local MPPT. The error between the reference provided by the MPPT and the PV voltage/current is minimized by adjusting the shoot through duty cycle in the corresponding submodule D_i using a PI controller [9].

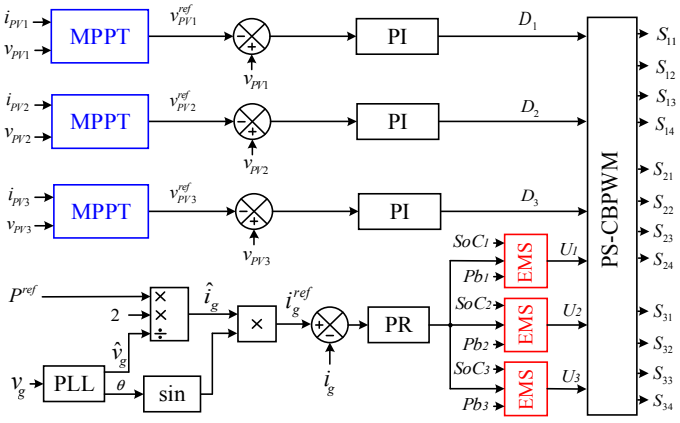

Fig. 3. Schematic of the conventional control of the battery assisted CM-qZSI for PV systems.

IV. Proposed MPC for the Cascaded Multilevel Quasi Z-source Inverter with Battery Storage

MPC in power electronics has several advantages, such as: easy implementation, constraints inclusion in nonlinear systems, and high accuracy and fast dynamic response [13]-[16]. A thorough analysis of MPC approach and its characteristics can be found in [16]. The most well-known class of MPC in power electronics is finite control set (FCS) MPC. FCS-MPC is summarized in the following tasks:

1- References estimation.
2- Prediction model.
3- Cost function optimization.
4- Gating signals application.

However, since FCS-MPC predicts the future conduct of the controlled variable for all the possible switching states in each sampling time, it is computationally demanding [17]. Hence, a control algorithm with low computational demand for CM-qZSI has been proposed in this paper. In in the proposed control strategy, the grid current is controlled through a PR controller, while the PV and battery currents are controlled through MPC.

A) References estimation:

Since the converter used here is fed by PV panels, local maximum power point trackers are indispensable for making the PV panels provide their maximum available power continuously. The MPPTs cater the PV current/voltage references that should be set for such an operating condition. In this paper, the classical Perturb & Observe (P&O) is adopted.

The power delivered by each submodule is determined based on the energy management of the system. The latter considers the power required by the grid, the power withdrawn from the PV panels, and the SOC of the batteries. Hence, the references are going to be the PV current, the power injected to the grid P^{ref} and the battery current i_{bi}^{ref}. The battery current in each submodule can be estimated as:

$$i_{bi}^{ref}=\frac{P_{bi}}{v_{C2}} \tag{7}$$

where P_{bi} is the battery exchanged power in the *ith* submodule, which can be determined as follows

$$P_{bi}=P_i^{ref}-P_{pvi} \tag{8}$$

such as, P_{pvi} and P_i^{ref} are the power harvested and power reference in the i^{th} submodule, respectively. The total active power reference is considered to be divided equally among the total number of submodules in order to avoid the distortion of the current injected to the grid.

B) Prediction model:

The flowchart of the shoot through state generation in the proposed method is shown in Fig. 4. In order to control the PV and battery currents through MPC, the model of the dc-side of the system needs to be derived. This model can be obtained from the continuous-time equations of the inverter presented in the second section.

Since the average current going through the PV capacitor is zero, the PV current is estimated as the qZS network first

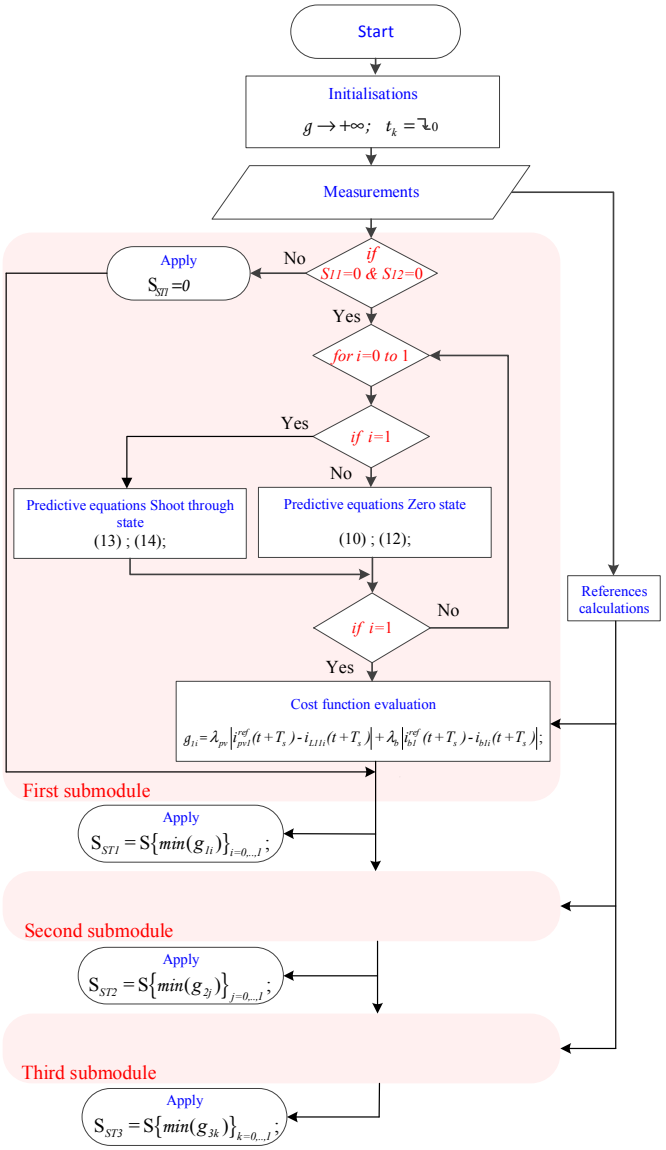

Fig. 4. Shoot through state generation in the proposed controller.

inductor's current. Both models of the system during zero state and shoot through state need to be taken into account.

1. Zero state, for deriving the predicted variables, usually, the approach of forward-difference Euler is used,

$$\frac{d\,x(t)}{dt} \approx \frac{x(t+T_s) - x(t)}{T_s} \tag{9}$$

where $x(t+T_s)$ and T_s are the estimated variable for the next sampling instant and the sampling time, respectively. By substituting (9) into the qZS network first inductor's current during the zero state (3), the predicted PV current can be found as follows:

$$i_{PVi}(t+T_s) = i_{PVi}(t) + \frac{T_s}{L_1}\left(v_{pvi}(t) - i_{PVi}(t) r_{L1} - v_{C1i}(t)\right) \tag{10}$$

The battery current is estimated as the difference between the qZS network's currents,

$$i_{bi} = i_{L2i} - i_{L1i} \tag{11}$$

Hence, the predicted battery current can be estimated as follows

$$i_{bi}(t+T_s) = i_{L2i}(t) - \frac{T_s}{L_2} v_{C2i} - i_{PVi}(t+T_s) \tag{12}$$

2. Shoot through state, by substituting (9) into the qZS network first inductor's current during the shoot through state (5), the predicted PV current can be found similarly as follows,

$$i_{PVi}(t+T_s) = i_{PVi}(t) + \frac{T_s}{L_1}\left(v_{pvi}(t) - i_{PVi}(t) r_{L1} + v_{C2i}(t)\right) \tag{13}$$

Then, the battery's predicted current in each submodule can be assessed as,

$$i_{bi}(t+T_s) = i_{L2i}(t) + \frac{T_s}{L_2} v_{C1i} - i_{PVi}(t+T_s) \tag{14}$$

C) Cost function optimization:

Among the advantages of MPC is its multivariable inclusion. All the controlled variables can be included in a single cost function, which in this paper are, the PV current, and the battery current. Hence, the cost function can be defined as,

$$g = \lambda_{pv} g_{pv} + \lambda_b g_b \tag{15}$$

where λ_{pv} and λ_b, are the weighting factors for PV current term, and the battery current. Their corresponding terms are written as follows,

$$g_{pv} = \left|i_{pv}^{ref}(t+T_s) - i_{pv}(t+T_s)\right|;\ g_b = \left|i_b^{ref}(t+T_s) - i_b(t+T_s)\right|;$$

D) Gating signals application:

The aforementioned cost function is calculated for both zero state and shoot through state and the switching state that minimizes the cost function should lead to the desired control objective. The prediction algorithm runs only if the current state is zero ($S1_i$=0 & $S2_i$=0), and if the minimized cost function corresponds to zero state then the system will continue in a zero state, otherwise, a shoot through state will be applied. The shoot through state is decided as a high logic value using the variable S_{ST}.

The grid current is controlled through a PR controller whose transfer function is expressed as:

$$H(s) = \frac{k\omega s}{s^2 + k\omega s + \omega^2} \tag{16}$$

where ω is the grid frequency, and k is the resonant gain. This transfer function can be discretized by using the Trapezoidal approach as the following [20]:

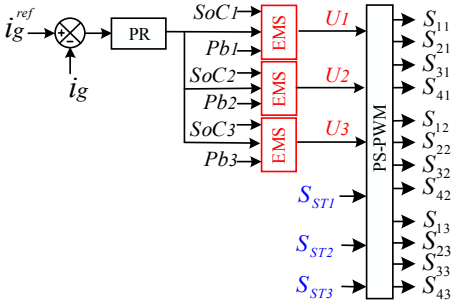

Fig. 6. Grid current regulation and switching state generation in the proposed controller.

TABLE I.
A COMPARAISON OF THE PROPOSED CONTROLLER WITH FCS-MPC IN TERMS OF THE NUMBER OF MATHEMATICAL OPERATIONS

Method			+ & –	×	÷
FCS-MPC	*Per iteration*		*18*	*11*	*3*
	27 iterations		***486***	***297***	***81***
Proposed controller	*Prediction model*	*Per cell*	*11*	*9*	*2*
		Per iteration	*33*	*27*	*6*
		2 iterations	*66*	*54*	*12*
	PR		*9*	*14*	*1*
			75	***68***	***13***

$$H(z)=\frac{x-xz^{-2}}{x+y+4-2(4-y)z^{-1}-(x-y-4)z^{-2}} \quad (17)$$

where $x=2k\omega T_s$ and $y=(\omega T_s)^2$. The grid current regulation and switching state generation in the proposed controller are sketched in Fig. 6.

V. COMPUTATIONAL EFFORT IN THE PROPOSED CONTROLLER

Table I shows a comparison between the proposed MPC controller and FCS-MPC in terms of the number of mathematical operations. The numbers in this table have been estimated as follows:

Proposed method: The equations used in this method are:
- -(10), (12), (13), and (14), which are for the PV and battery currents control;
- -(17) is employed for the grid current control;
- -A two terms cost function (15) for the optimization process.

FCS-MPC: This method uses:
- -(10), (12), (13), and (14) for the PV and battery current regulation;
- -(1) and (2) in its discretized form for the grid current control;
- -A three terms cost function.

As it can be seen from this table, the number of mathematical operation in the proposed method is 75 subtractions and addictions, 68 multiplications, and 13 divisions. Whereas, FCS-MPC algorithm performs 486 subtractions and addictions, 297 multiplications, and 81 divisions considering 27 iterations.

As it can be seen from Table I, the proposed method performs around 85% fewer mathematical operations with respect to the classical FCS-MPC in each sampling period.

VI. SIMULATION RESULTS AND DISCUSSION

A detailed simulation model of CM-qZS inverter conformable to the schematic shown in Fig. 1 has been developed for validating the theoretical analysis. The CM-qZS is fed by PV panels whose specifications were taken from the back of a real PV panel in the Lab (Universal Solar WXS230P-US). Under the standard test conditions (STC), these PV panels have: P_{MPP}=230W, I_{MPP}=7.52A, I_{sc}=8.56A, and v_{oc}=36.9V. To reach the desired voltage level, three PV panels were connected in series in each power module. The batteries were a lithium-ion type with a capacity of 6Ah and 24V nominal voltage. The qZ network passive elements were selected to be: L_1=L_2=0.6mH and C_1=C_2=2000μF. The filter inductor and stray resistance were 10mH and 0.1Ω, respectively. The switching frequency was f_{sw}=5kHz. The MPPTs were the conventional P&O [18]-[19], with a frequency and step size of 10Hz and Δv=0.5V (for the current ΔI=0.075A), respectively.

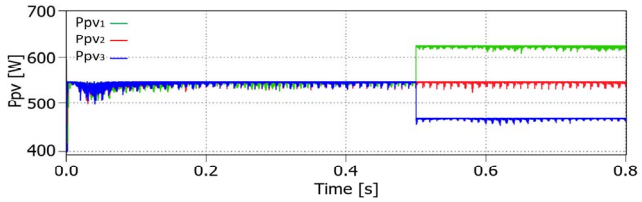

Fig. 7. The harvested PV power from the three cells by using the conventional PI linear controllers.

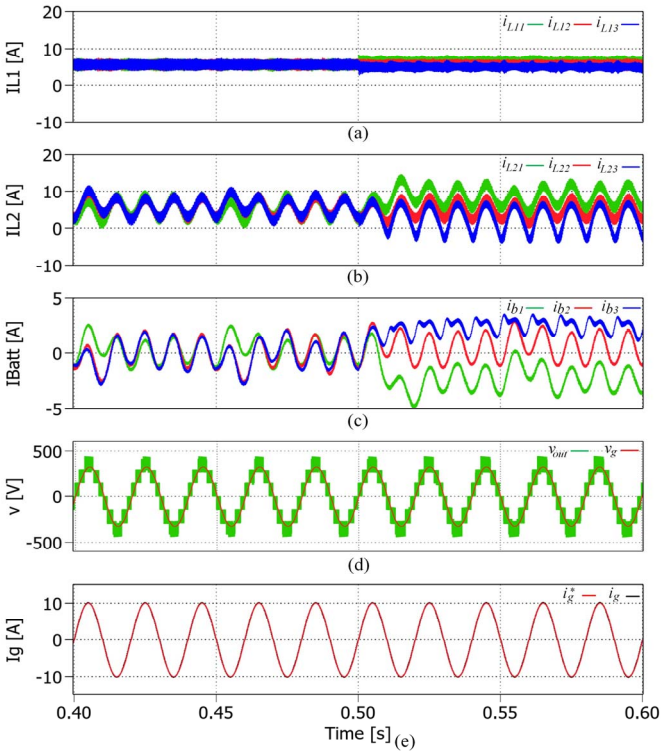

Fig. 8. Simulation results of the CM qZSI when the conventional linear PI controller is used, (a) the first qZ networks' inductor currents, (b) the second qZ networks' inductor currents, (c) the batteries current, (d) the output voltage, and (e) the current injected to the grid.

For the sake of comparison, the classical control of the CM-qZSI has been also tested and with the same parameters. The system has been tested under the same and different weather conditions among the power modules. The CM-qZSI starts with an average solar irradiance in all submodules and after 1.5s from the starting of the test, the irradiance increases in the first submodule and decreases in the third one. The irradiance in the second power module remains the same during the whole test. The results shown in Fig. 7 and Fig. 8 correspond to the conventional control of the CM-qZSI with linear PI controllers, whereas the ones shown in Fig. 9 and Fig 10 were obtained by the proposed control method.

As it can be seen from Fig. 8(c), the battery current in the conventional controller suffers from a double line-frequency

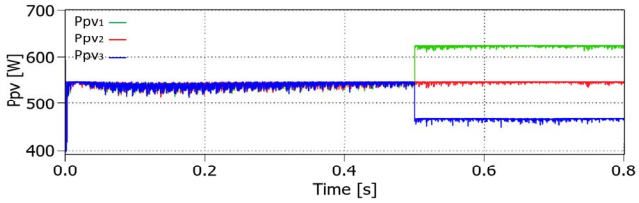

Fig. 9. The harvested PV power from the three cells by using the proposed MPC controller.

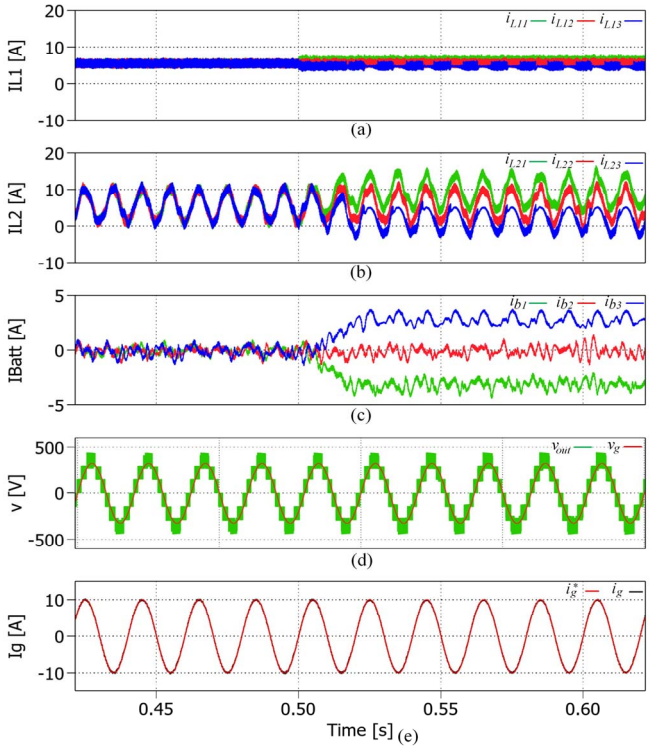

Fig 10. Simulation results of the CM qZSI when the proposed MPC controller is used, (a) the first qZ networks' inductor currents, (b) the second qZ networks' inductor currents, (c) the batteries current, (d) the output voltage, and (e) the current injected to the grid.

ripple. Its value was measured as Δi_b=3.39A. In contrast, in the proposed method this ripple has been reduced by almost three times (Δi_b=1.15A) since the battery current is directly controlled. One should note, that the double line-frequency ripple has been reduced at the expenses of the second qZ network's inductor current i_{L2} as well as the first qZ network's capacitor voltage.

VII. Conclusion

A model predictive-based control method for PV fed CM-qZSI with integrated energy storage has been proposed in this paper. The double line-frequency ripple in the battery current of CM-qZS inverter is a critical issue since it affects the battery life time. The battery current can be smoothened by using MPC; however, MPC is computationally demanding. In this paper, an MPC-based control strategy has been presented, where decreasing the battery current ripple as well as the computational burden were the main targets. As it has been shown in the obtained results, the battery current has been considerably reduced, while around 85% less processing power was applied compared to the conventional MPC.

VIII. References

[1] D. Karwatzki and A. Mertens, "Generalized Control Approach for a Class of Modular Multilevel Converter Topologies," *IEEE Trans. Power Electron.*, vol. 33, no. 4, pp. 2888-2900, April 2018.

[2] A. Lashab, D. Sera, J. Martins and J. M. Guerrero, "Multilevel DC-Link Converter-Based Photovoltaic System with Integrated Energy Storage," 2018 *5th International Symposium on Environment-Friendly Energies and Applications* (EFEA), Rome, 2018, pp. 1-6.

[3] J. Kucka, D. Karwatzki and A. Mertens, "Enhancing the Reliability of Modular Multilevel Converters Using Neutral Shift," *IEEE Trans. Power Electron.*, vol. 32, no. 12, pp. 8953-8957, Dec. 2017.

[4] Y. Liu, B. Ge and H. Abu-Rub, "Modelling and controller design of quasi-Z-source cascaded multilevel inverter-based three-phase grid-tie photovoltaic power system," *in IET Renewable Power Generation*, vol. 8, no. 8, pp. 925-936, 11 2014.

[5] Y. Liu, B. Ge, H. Abu-Rub and F. Z. Peng, "An Effective Control Method for Three-Phase Quasi-Z-Source Cascaded Multilevel Inverter Based Grid-Tie Photovoltaic Power System," *IEEE Trans. Ind. Electron.*, vol. 61, no. 12, pp. 6794-6802, Dec. 2014.

[6] Y. Liu, B. Ge and H. Abu-Rub, "An active power decoupling quasi-Z-source cascaded multilevel inverter," *IECON 42nd Annu. Conf. of the IEEE Industrial Electronics Society,* Florence, 2016, pp. 6453-6458.

[7] R. Zhang, Y. Li and Y. Liu, "Constraints and control strategies of quasi-Z-source cascaded multilevel inverter," IECON *43rd Annu. Conf. of the IEEE Industrial Electronics Society*, Beijing, 2017, pp. 4209-4214.

[8] A. Gorgani, M. Elbuluk, Y. Sozer and H. A. Rub, "Quasi-Z-source-based multilevel inverter for single phase PV applications," *2016 IEEE Energy Conversion Congress and Exposition (ECCE),* Milwaukee, 2016, pp. 1-7.

[9] D. Sun *et al*., "An Energy Stored Quasi-Z-Source Cascade Multilevel Inverter-Based Photovoltaic Power Generation System," *IEEE Trans. Ind. Electron.*, vol. 62, no. 9, pp. 5458-5467, Sept. 2015.

[10] P. Iniyaval and S. R. Karthikeyan, "Fuzzy logic based quasi Z-source cascaded multilevel inverter with energy storage for photovoltaic power generation system," *Inter. Conf. on Emerging Trends in Engineering, Technology and Science (ICETETS)*, Pudukkottai, 2016, pp. 1-5.

[11] B. Ge, Y. Liu, H. Abu-Rub and F. Z. Peng, "State-of-Charge Balancing Control for a Battery-Energy-Stored Quasi-Z-Source Cascaded-Multilevel-Inverter-Based Photovoltaic Power System," *IEEE Trans. Ind. Electron.*, vol. 65, no. 3, pp. 2268-2279, March 2018.

[12] J. G. Cintron-Rivera, Y. Li, S. Jiang, and F. Z. Peng, "Quasi-Z-Source inverter with energy storage for Photovoltaic power generation systems," *in 26th proc. IEEE. APEC. Illinois*, pp. 401-406, 2011.

[13] A. Lashab, D. Sera, J. M. Guerrero, L. Mathe and A. Bouzid, "Discrete Model-Predictive-Control-Based Maximum Power Point Tracking for PV Systems: Overview and Evaluation," *IEEE Trans. Power Electron.*, vol. 33, no. 8, pp. 7273-7287, Aug. 2018.

[14] A. Lashab, D. Sera, J. Martins and J. M. Guerrero, "Model Predictive-Based Direct Battery Control in PV Fed Quasi Z-Source Inverters," 2018 *5th International Symposium on Environment-Friendly Energies and Applications* (EFEA), Rome, 2018, pp. 1-6.

[15] M. Rivera, V. Yaramasu, A. Llor, J. Rodriguez, B. Wu, and M. Fadel, "Digital predictive current control of a three-phase four-leg inverter," *IEEE Trans. Ind. Electron.*, vol. 60, no. 11, pp. 4903–4912, 2013.

[16] S. Vazquez *et al.*, "Model predictive control: A review of its applications in power electronics," *IEEE Ind. Electron. Mag.*, vol. 8, no. 1, pp. 16–31, 2014.

[17] P. Cortes, A. Wilson, S. Kouro, J. Rodriguez, and H. Abu-Rub, "Model predictive control of multilevel cascaded H-bridge inverters," *IEEE Trans. Ind. Electron.*, vol. 57, no. 8, pp. 2691–2699, 2010.

[18] H. Snani, M. Amarouayache, A. Bouzid, A. Lashab and H. Bounechba, "A study of dynamic behaviour performance of DC/DC boost converter used in the photovoltaic system," 2015 IEEE *15th International*

Conference on Environment and Electrical Engineering (EEEIC), Rome, 2015, pp. 1966-1971.

[19] H. Bounechba, A. Bouzid, H. Snani, and A. Lashab, “Electrical Power and Energy Systems Real time simulation of MPPT algorithms for PV energy system,” *Int. J. Electr. Power Energy Syst.*, vol. 83, pp. 67–78, 2016.

[20] M. Ciobotaru, R. Teodorescu and F. Blaabjerg, "A new single-phase PLL structure based on second order generalized integrator," 2006 *37th IEEE Power Electronics Specialists Conference*, Jeju, 2006, pp. 1-6.